

# Cr Doped TiO<sub>2</sub> Supported on TUD-1 Photocatalyst for Dye Photodegradation

Ooi Yee Khai<sup>a</sup>, Leny Yulianti<sup>b</sup>, Siew Ling Lee<sup>b\*</sup>

<sup>a</sup>Department of Chemistry, Faculty of Science, Universiti Teknologi Malaysia, 81310 UTM Johor Bahru, Johor, Malaysia

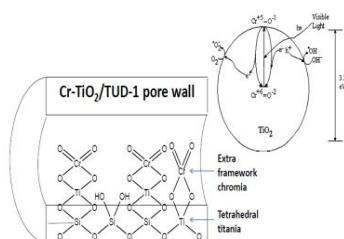
<sup>b</sup>Ibnu Sina Institute for Fundamental Science Studies, Universiti Teknologi Malaysia, 81310 UTM Johor Bahru, Johor, Malaysia

\*Corresponding author: sllee@ibnusina.utm.my

## Article history

Received :5 March 2014  
Received in revised form :  
19 April 2014  
Accepted :3 May 2014

## Graphical abstract



## Abstract

New visible light driven photocatalysts of 1 mol% Cr doped TiO<sub>2</sub> supported on TUD-1 have been successfully synthesized. The Cr-TiO<sub>2</sub>/xTUD-1 (x = 10, 20, 30, 40 and 50) photocatalysts were prepared via surfactant-free sol-gel method followed by wet impregnation procedures. XRD analysis revealed that both TiO<sub>2</sub> and Cr were incorporated in the highly porous siliceous matrix. FTIR analysis showed the existence of Si-O-Ti in all the materials. As observed, tetrahedral-coordinated Ti species were dominant in Cr-TiO<sub>2</sub>/10TUD-1, Cr-TiO<sub>2</sub>/20TUD-1 and Cr-TiO<sub>2</sub>/30TUD-1. Meanwhile, octahedral-coordinated Ti species were the dominant species in Cr-TiO<sub>2</sub>/40TUD-1 and Cr-TiO<sub>2</sub>/50TUD-1. It has been demonstrated that the amount of TUD-1 as photocatalyst support affected the wavelength response and the bandgap energy of the resulting materials. All the materials have bandgap energy of ~2.9 eV. The photocatalytic performance of the synthesized materials was tested out in dye photodegradation under visible light irradiation at 298 K for 5 hours. Results showed that all Cr-TiO<sub>2</sub>/TUD-1 materials had higher photocatalytic activity than that of Cr-TiO<sub>2</sub>. This could be explained by the high surface area and porosity provided by TUD-1 in enhancing the adsorption and diffusivities of the dye molecules, hence leading to the promising photocatalytic activity. Among the materials prepared, Cr-TiO<sub>2</sub>/30TUD-1 appeared as the most superior photocatalyst which gave the highest dye photodegradation.

**Keywords:** TUD-1; photocatalyst; titania; dye degradation

## Abstrak

Fotomangkin dengan pacuan cahaya nampak daripada 1 mol% Cr dop TiO<sub>2</sub> disokong atas TUD-1 telah berjaya disintesis. Fotomangkin Cr-TiO<sub>2</sub>/xTUD-1 (x = 10, 20, 30, 40 and 50) telah dihasilkan melalui kaedah sol-gel tanpa surfaktan diikuti dengan kaedah penresapan basah. Analisis XRD menunjukkan bahawa TiO<sub>2</sub> dan Cr telah bergabung dalam matrik silika yang berliang tinggi. Analisis FTIR menunjukkan kewujudan Si-O-Ti dalam semua sampel. Spesies dominan dalam Cr-TiO<sub>2</sub>/10TUD-1, Cr-TiO<sub>2</sub>/20TUD-1 dan Cr-TiO<sub>2</sub>/30TUD-1 adalah Ti berstruktur koordinat tetrahedron, manakala spesies dominan dalam Cr-TiO<sub>2</sub>/40TUD-1 dan Cr-TiO<sub>2</sub>/50TUD-1 adalah Ti berstruktur koordinat oktahedron. Amaun TUD-1 digunakan sebagai sokongan fotomangkin mempengaruhi respon panjang gelombang dan jurang jalur tenaga fotomangkin. Semua sampel mempunyai jurang jalur tenaga sebanyak ~2.9 eV. Fotodegradasi pewarna menggunakan sinaran cahaya ketara pada 298 K selama 5 jam telah dijalankan untuk menguji prestasi pemangkinan. Adalah dibuktikan bahawa, semua sampel Cr-TiO<sub>2</sub>/TUD-1 mempunyai aktiviti yang lebih tinggi berbanding Cr-TiO<sub>2</sub>. Ini disebabkan TUD-1 mempunyai luas permukaan dan keliangan yang tinggi, justeru membawa kepada peningkatan penjerapan dan kemesapan molekul pewarna. Antara sampel yang dihasilkan, Cr-TiO<sub>2</sub>/30TUD-1 merupakan fotomangkin yang paling unggul untuk menfotodegradasikan perwarna.

**Kata kunci:** TUD-1; fotomangkin; titanium dioksida; degradasi pewarna

© 2014 Penerbit UTM Press. All rights reserved.

## 1.0 INTRODUCTION

Dye pollution has always been a serious issue around the globe. Dyes are deposited into rivers and streams thus causing depletion to the water sources available for daily usage and drinking. The effluents have been handled with several chemical and physical procedures such as adsorption, precipitation, flocculation and reverse osmosis but these are non-destructive techniques [1]. TiO<sub>2</sub>-based photocatalysts have high efficiency in degradation of trace elements of organic substances in contaminated air and wastewater [2, 3]. They utilize advanced oxidation processes (AOPs) that involve total elimination of organic contaminants through generation of hydroxyl radicals, <sup>•</sup>OH. These radicals are effective and non-selective oxidant species that are capable of degrading dangerous organic chemicals into CO<sub>2</sub>, H<sub>2</sub>O and simple acids [4]. The most thermodynamically steadfast crystalline TiO<sub>2</sub> has two polymorph forms which are rutile and anatase, where rutile is the more thermodynamically stable form, with bandgap energy of 3.02 eV and 3.20 eV for anatase. However, TiO<sub>2</sub> is not an efficient photocatalyst because of its large bandgap energy that only allows operation within ultraviolet range and high electron-hole recombination rate which retains a limited amount of hydroxyl species on its surface. Besides that, its low surface area (~50 m<sup>2</sup>/g) has been a major disadvantage [5].

In order to solve these problems, modifications of TiO<sub>2</sub> such as coupling with noble metals as co-catalyst, transition metal oxides and non-metal doping have been carried out [3]. Apart from that, dye sensitization and usage of large surface area silica support to improve the photocatalytic performance of TiO<sub>2</sub> have also been intensively studied. Metal ion doped TiO<sub>2</sub> seemed to be more photoactive than the bare TiO<sub>2</sub>. Recently, as ways to improve the photocatalytic activity of titania, chromium doping has proven as a likely strategy [6]. Cr<sup>6+</sup> is chosen as the doping transition metal due to its vast positive reduction potential that can assist in suppressing the recombination of photogenerated electron-holes and increasing the charge separation can cause increment in the wavelength response range. Nevertheless, the surface area and porosity remains unclarified since surface area plays a major part in the adsorption and degradation processes in catalyst. Support provides larger surface area and better porosity, which further facilitates diffusibility and adsorption of substrate.

Silica is inert, non-toxic, environmentally friendly, and can be found abundantly in the earth's crust, or commonly found as sand or quartz. It has been proven to be an excellent support for different materials *e.g.* metal oxides and non-metals [5]. The discovery of TS-1 by Shell Company in 1971 where Ti was substituted by Si in MFI framework has led to the usage of silica support as one of the modification methods for TiO<sub>2</sub>. A series of materials containing highly dispersed titanium centers in a silica matrix such as Ti-silica aerogel and Ti-fumed silica have been reported. It is established that nanoscale engineering of sol-gel TiO<sub>2</sub>-SiO<sub>2</sub> mixed oxides provides excellent photocatalytic activity. It was also observed that SiO<sub>2</sub> was an excellent support for transition metal ion doped TiO<sub>2</sub>. Nevertheless, there is still absence of direct experimental evidence on the silica support towards the photocatalytic activity of TiO<sub>2</sub> and the physico-chemical relationship between TiO<sub>2</sub> and SiO<sub>2</sub> has also yet to be clarified.

MCM-41, SBA-15, silica aerogel, *etc.* are normally used as supports due to their high surface area. However, there are limitations to the supports mentioned such as low hydrothermal stability, thin walls, usage of templates causing impurities, time consuming, costly synthesis process and one-dimensional pore arrangement that limited their performance. Although doping

with transition metal has increased its usability to work under visible light, but the research on the role of support in photocatalyst design is still unclear as whether the support promotes or hinders the photocatalytic activity.

Similar to other mesoporous materials, Technische Universiteit Delft, TUD-1 has high surface area of 1000 – 1200 m<sup>2</sup>/g and excellent thermal resistance, which permits all kinds of catalyzed reactions to be managed up to 873 K. This novel material was first reported by T. Maschmeyer in 2001. TUD-1 exhibits high surface area of 400 – 1000 m<sup>2</sup>/g and thick mesoporous walls. It also has excellent thermal, hydrothermal and mechanical stability, tunable mesopore size distribution (pore volumes of 0.3 – 2.5 cm<sup>3</sup>/g), diameters of 25 – 250 Å and a random, three-dimensional interconnecting pores [6]. Therefore, TUD-1 shows more potential as photocatalyst support compared to the well reported support such as MCM-41 and SBA-15.

The three-dimensional sponge-like mesoporous material TUD-1 is straightforward to prepare. In fact, its synthesis procedure can readily be modified to introduce metals into the framework of TUD-1, imparting many different catalytic activities. Metal doped-TUD-1 catalysts have been proven to be very active, unlimited by diffusion and very stable [6]. In addition, TUD-1 was proven to be an excellent carrier material for catalysts in redox-, acid- and photocatalysis, enabling new applications. Unfortunately, report on the usage of TUD-1 showing the mesoporous structure support such as TUD-1 with different mol ratio and how does it affect the crystallinity morphology, surface area, and porosity of the photocatalyst remains very limited in photocatalytic design.

In this study, a series of photocatalyst supported on TUD-1 with different physical properties such as crystallinity, surface area and porosity are synthesized. This is essential in order to explore the important role and effect of support on the performance of the photocatalysts. Here, we report the physical-chemical properties and photocatalytic performance of Cr-TiO<sub>2</sub>/xTUD-1 in the photodegradation of dyes.

## 2.0 EXPERIMENTAL

### 2.1 Preparation of Photocatalysts

Three types of photocatalysts: TiO<sub>2</sub>, Cr-TiO<sub>2</sub>, and Cr-TiO<sub>2</sub>/xTUD-1 with molar ratio of Ti : Si = 1 : 10, 20, 30, 40 and 50, were synthesized. In the synthesis of Cr-TiO<sub>2</sub>/xTUD-1, sol-gel and impregnation methods with minor modification were applied. All the samples were calcined at 923 K for 6 hours. All chemicals used were provided by Sigma-Aldrich.

#### 2.1.1 Synthesis of TiO<sub>2</sub>

Titania was synthesized via sol-gel method. Titanium tetraisopropoxide (TTIP) was mixed with absolute ethanol as the solvent and acetylacetone as the chelating agent according to the molar ratio of 1 : 100 : 2, respectively [7]. The mixture was stirred for 60 minutes at room temperature and dried at 353 K overnight, followed by calcination at 773 K for 6 h.

#### 2.1.2 Synthesis of Cr-TiO<sub>2</sub>

Chromium oxide doped titania, Cr-TiO<sub>2</sub>, was synthesized via sol-gel method. TTIP was mixed with absolute ethanol as the solvent and acetylacetone as the chelating agent according to the molar ratio of 1 : 100 : 2, respectively, to form solution A. Then solution A was stirred for 60 minutes at ambient temperature. In

another beaker, chromium acetylacetonate was dissolved in acetylacetone. It was added dropwise into solution A. The mixture was stirred for another 60 minutes at room temperature and was dried at 353 K for solvent evaporation. Later, the mixture was left overnight at 383 K, subsequently calcined at 773 K for 6 h.

### 2.1.3 Synthesis of Cr-TiO<sub>2</sub>/xTUD-1

TUD-1 was obtained through a homogeneous mixture via mixing tetraethylorthosilicate (TEOS), triethanolamine (TEA) and water at room temperature. Tetraethylammonium hydroxide (TEAOH) was added drop-wise to the above mixture under stirring. Then vigorous stirring was continued until gelation of the synthesis mixture. In particular, the final synthesis gel has the molar composition of TEOS: 0.5 TEA: 0.1 TEAOH: 11H<sub>2</sub>O. After aging and drying in air, the mixture was solidified and formed a homogeneous gel. The solid gel was aged at room temperature for 6–24 h, dried at 473 K in air for 24 h, heated in an autoclave at 543 K for 2–24 h and finally calcined at 873 K in air for 16 h. TEOS was added with distilled water whilst stirring with solid Cr-TiO<sub>2</sub> before drop-wise addition of TEA and TEAOH via wet impregnation method.

## 2.2 Samples Characterization

X-ray diffraction (XRD) patterns were obtained with a Bruker Advance D8 transmission diffractometer using the Cu K<sub>α</sub> ( $\lambda = 1.5406 \text{ \AA}$ ) radiation as the diffracted monochromatic beam at 40 kV and 40 mA. The patterns were scanned in the  $2\theta$  range of 2 and 60° at a step of 0.050° and step time of 1 s. Diffuse reflectance ultra violet-visible (DR UV–vis) spectra were recorded under ambient conditions using a Perkin-Elmer Lambda 900 UV/VIS/NIR spectrometer and monitored in the range of 190–600 nm. Infrared (IR) spectra of the samples were collected on a Perkin-Elmer Fourier transform infrared (FTIR) spectrometer using KBr technique, with a spectral resolution of 2 cm<sup>-1</sup>, scans of 10 s, at temperature of 20 °C. Nitrogen adsorption-desorption isotherms were measured at 77 K using a Micromeritics ASAP 2020 V4.00 instrument. The surface area was calculated using the Brunauer, Emmett and Teller (BET) model.

### 2.3 Photocatalytic Testing

Prior to the photocatalytic testing, a solution containing 0.1 g of the photocatalyst, 100 mL of 150 ppm methylene blue was kept in dark to allow occurrence of physical adsorption, if any. Photodegradation of methylene blue was carried out at room temperature under irradiation of visible light for 5 hours with 550 W tungsten halogen lamps under constant stirring.

## 3.0 RESULTS AND DISCUSSION

### 3.1 X-Ray Diffraction (XRD) Analysis

The synthesized materials, Cr-TiO<sub>2</sub>/TUD-1 appeared to be as brownish fine powder. XRD patterns of the prepared Cr-TiO<sub>2</sub> and Cr-TiO<sub>2</sub>/xTUD-1 samples with various molar ratios of Si/Ti

are shown in Figure 1. As observed, Cr-TiO<sub>2</sub> shows both anatase and rutile crystalline phases (JCPDS 21-1272 and 21-1276, respectively). However, no apparent peaks were observed after being supported onto TUD-1, indicating the materials were in amorphous form. The results may also imply that Cr-TiO<sub>2</sub> was well dispersed onto the TUD-1.

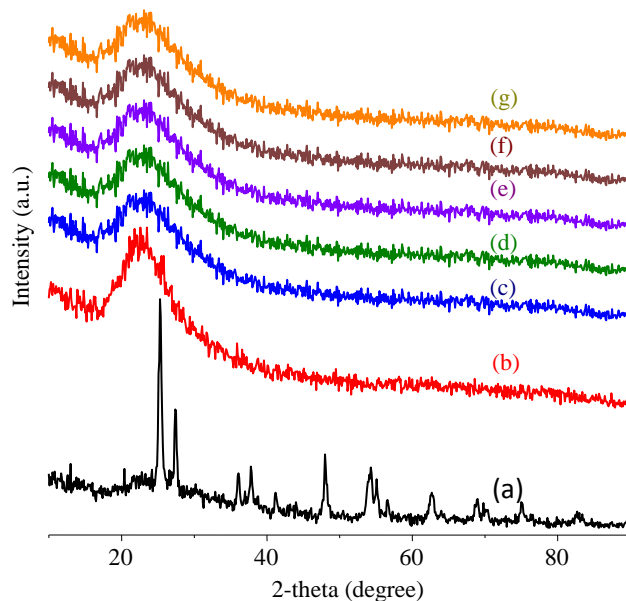


**Figure 1** XRD patterns of (a) Cr-TiO<sub>2</sub>, (b) Cr-TiO<sub>2</sub>/10TUD-1, (c) Cr-TiO<sub>2</sub>/20TUD-1, (d) Cr-TiO<sub>2</sub>/30TUD-1, (e) Cr-TiO<sub>2</sub>/40TUD-1, (f) Cr-TiO<sub>2</sub>/50TUD-1 and (g) TUD-1

### 3.3 BET Surface Area and Nitrogen Adsorption-Desorption Isotherm

As shown in Figure 2, both TiO<sub>2</sub> and Cr-TiO<sub>2</sub> have type IV isotherm, which is characteristics of mesoporous materials. The isotherm plot also suggested that these materials are mesoporous material with H3 pore type, with slit-shaped and non-uniform pores due to the removal of organic matters during calcination. Observation of ‘low knee’ region at the range  $p/p_0 < 0.1$  in the isotherm plot indicates the existence of macropores. The monolayer adsorption of nitrogen occurred at  $p/p_0 < 0.45$ . The Figures 2(a) and 2(b) show a sharp step capillary condensation in mesopores region ( $p/p_0 = 0.45-0.9$ ), suggesting a narrow pore size distribution [9].

At  $p/p_0 = 0.5$ , the accessible pores are totally filled with adsorbate and the isotherm reaches a plateau that remains fairly invariant as  $p/p_0$  approaches unity. As depicted in Figure 2(c), the nitrogen sorption isotherm of Cr-TiO<sub>2</sub>/30TUD-1 is of type IV, strongly indicating the presence of mesopores in the material [5]. The total mesopore volume was calculated from the amount of vapour adsorbed at  $p/p_0 = 0.50$ ; assuming that Cr-TiO<sub>2</sub>/30TUD-1 was then filled with condensed liquid nitrogen in the normal liquid state.

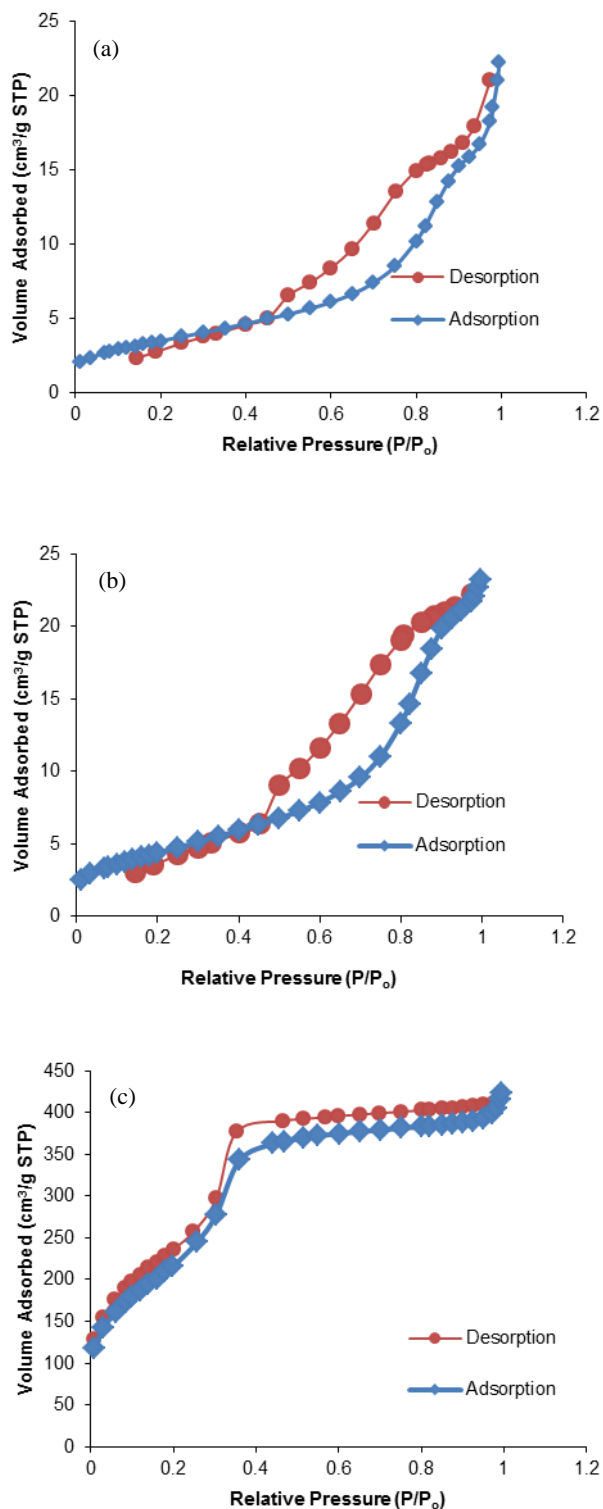


**Figure 2** Isotherms of (a) TiO<sub>2</sub>, (b) Cr-TiO<sub>2</sub>, and (c) Cr-TiO<sub>2</sub>/30TUD-1

Adsorption at low pressure ( $p/p_0 < 0.25$ ) is accounted for by monolayer-multilayer adsorption of N<sub>2</sub> on the wall of mesopores. Similarly, the figure shows a sharp step capillary condensation in mesopores region ( $p/p_0 = 0.3-0.4$ ), suggesting a narrow pore size distribution. Hysteresis in both the lower ( $p/p_0 = 0.1-0.4$ ) H2 hysteresis and higher ( $p/p_0 = 0.9-1.0$ ) H3

hysteresis pressure region is caused by particles porosity or by significant larger macropores. The absence of this hysteresis loops in the capillary condensation range is an indication that the material possesses pores in a lower mesopore range. Table 1 shows the measurement of the BET surface area and pore volume of TiO<sub>2</sub>, Cr-TiO<sub>2</sub> and Cr-TiO<sub>2</sub>/30TUD-1 samples. Apparently, both the surface area and the pore volume of Cr-TiO<sub>2</sub> increased significantly after loading on TUD-1. The increment of surface area and pore volume was 54 and 19 times, respectively.

**Table 1** Surface area and pore volume of TiO<sub>2</sub>, Cr-TiO<sub>2</sub>, and Cr-TiO<sub>2</sub>/30TUD-1

Samples	Surface area (m <sup>2</sup> /g)	Pore volume (cm <sup>3</sup> /g)
TiO <sub>2</sub>	12.8	0.028
Cr-TiO <sub>2</sub>	16.2	0.034
Cr-TiO <sub>2</sub> /30TUD-1	864.3	0.637

### 3.4 Diffused Reflectance Ultraviolet-Visible (DRUV-Vis) Analysis

The Figure 3 shows the UV-Visible DR spectra of chromium doped TiO<sub>2</sub> supported on TUD-1 materials.

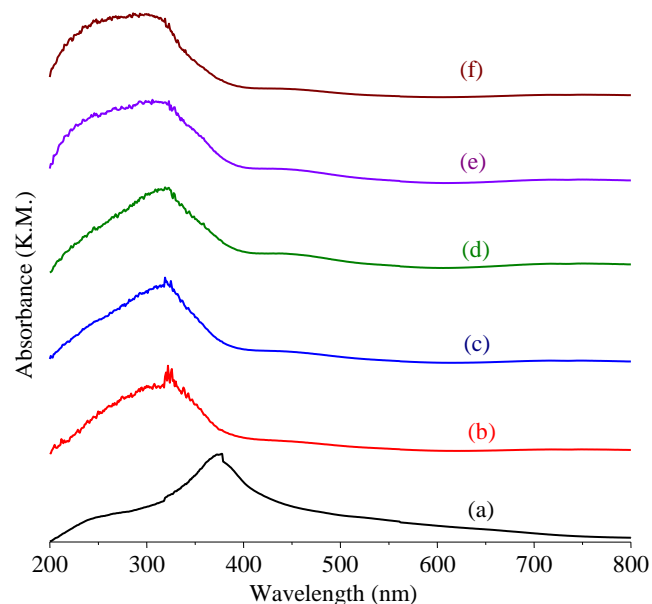


**Figure 3** DR UV-Vis spectra of (a) Cr-TiO<sub>2</sub>, (b) Cr-TiO<sub>2</sub>/10TUD-1, (c) Cr-TiO<sub>2</sub>/20TUD-1, (d) Cr-TiO<sub>2</sub>/30TUD-1, (e) Cr-TiO<sub>2</sub>/40TUD-1, and (f) Cr-TiO<sub>2</sub>/50TUD-1

Cr-TiO<sub>2</sub> has a dominant peak at 380 nm which might be attributed to the octahedrally coordinated Ti species in the sample [10]. Meanwhile, the peak around 200–300 nm was due to isolated tetrahedral framework Ti or Cr species. The broad adsorption peak in range 400–800 nm was associated to the presence of Cr. As observed, the addition of TUD-1 has caused blue shifting in the spectra. The transition metal doping created an occupied level in the band gap that enabled the photocatalyst to perform under visible light. The calculated band gap energies of the TUD-1 supported Cr-TiO<sub>2</sub> are summarized in Table 2. From the band edge of the sample series, it is observed that due to the low concentration of chromium (0.03 wt% in total), the

Cr-TiO<sub>2</sub> was incorporated homogeneously with even dispersion onto the surface of TUD-1. With increasing amount of TUD-1, the percentage of Cr in the samples was lesser, hence, resulted in the increase of band gap energy. The decrease of Cr could also be visualised by the remarkably reduced intensity of the adsorption peaks at 400–800 nm in these TUD-1 supported Cr-TiO<sub>2</sub> samples (Figure 3).

**Table 2** Bandgap energy of Cr-TiO<sub>2</sub> and Cr-TiO<sub>2</sub>/xTUD-1 (x = 10, 20, 30, 40, and 50)

Samples	Band edge (nm)	Band gap (eV)
Cr-TiO <sub>2</sub>	500	2.47
Cr-TiO <sub>2</sub> /10TUD-1	410	3.02
Cr-TiO <sub>2</sub> /20TUD-1	400	3.10
Cr-TiO <sub>2</sub> /30TUD-1	390	3.18
Cr-TiO <sub>2</sub> /40TUD-1	380	3.26
Cr-TiO <sub>2</sub> /50TUD-1	370	3.35

### 3.5 Photocatalytic Testing

Photocatalytic activity of the materials was evaluated through the photodegradation of methylene blue under visible light at room temperature. From Figure 4, it was observed that the photocatalytic degradations by all of the TUD-1 supported Cr-TiO<sub>2</sub> samples were higher than that of Cr-TiO<sub>2</sub>. The highest photocatalytic degradation was reached when Cr-TiO<sub>2</sub>/30TUD-1 was used as the photocatalyst. The functionality of the support material, TUD-1, was proven by increasing 3-fold of the photocatalytic conversion of methylene blue compared to bare Cr-TiO<sub>2</sub>. The results strongly suggested that large surface area and high pore volume in the samples have facilitated in the dye photodegradation. The photodegradation percentage was slightly decreased when higher amount of TUD-1 was used in Cr-TiO<sub>2</sub>/40TUD-1 and Cr-TiO<sub>2</sub>/50TUD-1. The phenomena could be explained by the possible trapping of Cr-TiO<sub>2</sub> in the excess silica matrix, preventing the substrate from coming into contact with the active sites, which are available in Cr-TiO<sub>2</sub>. Besides, the large amount of silica support may have limited the accessibility to the active sites.

For samples with less amount of TUD-1, the Cr-TiO<sub>2</sub> was not dispersed well onto the silica matrix, resulting in agglomeration. Consequently, the active sites for the photodegradation of dyes were reduced. Obviously, all the TUD-1 supported Cr-TiO<sub>2</sub> has better photocatalytic performance than that of Cr-TiO<sub>2</sub>. This strongly indicates that the silica support is crucial to provide dispersion centre, which is able to prevent obstruction in the accessibility of the Cr-TiO<sub>2</sub> active sites [12]. In the photocatalytic degradation of dyes, the band gap energy does not play a significant role where the photocatalytic activity is strongly dependent on surface area of the material by using TUD-1 as support which provides better distribution of active sites and reactant diffusivities.

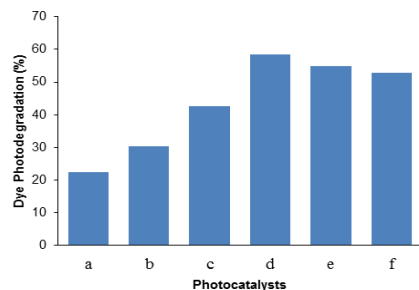


**Figure 4** Photodegradation percentage of methylene blue using (a) Cr-TiO<sub>2</sub>, (b) Cr-TiO<sub>2</sub>/10TUD-1, (c) Cr-TiO<sub>2</sub>/20TUD-1, (d) Cr-TiO<sub>2</sub>/30TUD-1, (e) Cr-TiO<sub>2</sub>/40TUD-1 and (f) Cr-TiO<sub>2</sub>/50TUD-1

In order to further understand the interaction between the photocatalyst and the substrate, photodegradation of basic and acidic dyes was carried out under the same condition. The initial concentration of each dye was 150 ppm. As can be seen, Cr-TiO<sub>2</sub>/30TUD-1 photocatalyst showed higher photocatalytic activity towards both the cationic dyes (methylene blue and malachite green) due to the negative charged deprotonated silanol (-SiOH) groups on the surface of TUD-1, which provided better interaction with the cationic dyes. The silanol group tends to repel anionic dyes (congo red and methyl orange) due to its negatively charged nature, hence weaker interaction is observed [12].

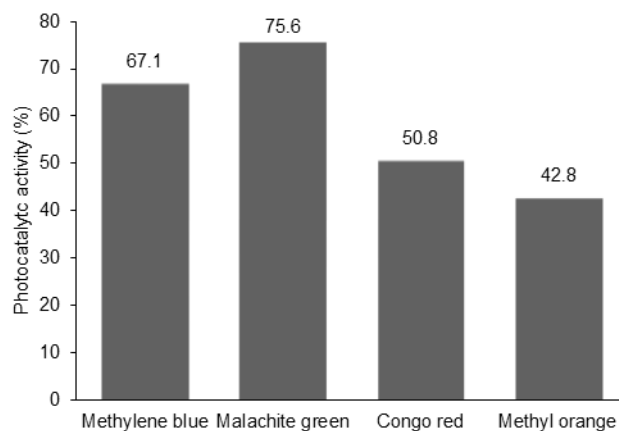


**Figure 5** Photodegradation of various dyes using Cr-TiO<sub>2</sub>/30TUD-1

### 4.0 CONCLUSION

The photocatalytic activity of Cr-TiO<sub>2</sub> under visible light irradiation was significantly enhanced after supporting on TUD-1. The highest photodegradation of methylene blue was achieved by Cr-TiO<sub>2</sub>/30TUD-1. Based on the results obtained, TUD-1 could be a promising photocatalyst support. It has also been demonstrated that Cr-TiO<sub>2</sub>/30TUD-1 has better photocatalytic degradation towards basic dyes instead of acidic dyes.

### Acknowledgement

The authors thank Universiti Teknologi Malaysia (UTM), Malaysia for characterization facilities and also Prof. Dr. Hadi Nur for the guidance. The authors also thank Ministry of Higher Education (MOHE) through Research University Grant Scheme (Vote No. QJ130000.2526.03H90) for the financial supports. Ooi Yee Khai also acknowledges the financial support from UTM through UTM Zamalah Scholarship [UTM.J.10.01/13.14/1/127/1(891129025295)].

### References

- [1] P. S. Keng, S. L. Lee, S. T. Ha, Y. T. Hung and S. T. Ong. 2013. REVIEW: Removal of Hazardous Pollutants from Aqueous Environment by Low Cost Adsorption Materials. *Environ. Chem. Lett.* 12: 15–25.
- [2] T. Z. Tong, J. L. Zhang, B. Z. Tian, F. Chen, D. N. He. 2008. Preparation of Fe<sup>3+</sup>-doped TiO<sub>2</sub> Catalysts by Controlled Hydrolysis of Titanium Alkoxide and Study on Their Photocatalytic Activity for Methyl Orange Degradation. *J. Hazard. Mater.* 155: 572–579.

- [3] T. Al. Ouafa, T.N. Quang, R. Touria. 2009. Preparation and Characterization of a New  $\text{TiO}_2/\text{SiO}_2$  Composite Catalyst for Photocatalytic Degradation of Indigo Carmin. *Environ. Chem. Lett.* 7: 175–181.
- [4] S. Quorzal, N. Barka, M. Tamimi, A. Assabbane, A. Nounah, A. Ihlal, Y. Ait-Ichou. 2009. Sol-gel Synthesis of  $\text{TiO}_2\text{-SiO}_2$  Photocatalyst for  $\beta$ -Naphthol Photodegradation. *Mater. Sci. Eng. C.* 29: 1616–1620.
- [5] M. Zhang, L. Shi, S. Yuan, J. Fang. 2009. Synthesis and Photocatalytic Properties of Highly Stable and Neutral  $\text{TiO}_2/\text{SiO}_2$  Hydrosol. *J. Colloid Interf. Sci.* 330: 113–118.
- [6] P. Atkins, J. D. Paula, 2006. *Atkin's Physical Chemistry*. eighth ed. Oxford University Press Inc. New York.
- [7] S. Neatu. 2009.  $\text{M/TiO}_2/\text{SiO}_2$  (M = Fe, Mn and V) Catalysts in Photodecomposition of Sulfur Mustard. *Appl. Catal. B Environ.* 91: 546–553.
- [8] R. F. Chen, C. X. Zhang, J. Deng, G. Q. Song. 2012. Preparation and Photocatalytic activity of  $\text{Cu}^{2+}$ -doped  $\text{TiO}_2/\text{SiO}_2$ . *International Journal of Minerals. J. Cryst. Growth.* 229: 428–432.
- [9] H. Hamdan, S. L. Lee, Y. Y. Tan, Mohd Nazlan Muhid. 2009. Visible Light Enable V and Cr Doped Titania-silica Aerogel Photocatalyst. *International Journal of Chemical Reactor Engineering.* 7. Article A54.
- [10] P. G. Ali Mehrizad. 2009. Synthesis of Nanosized  $\text{TiO}_2$  Powder by Sol-Gel Method in Acidic Conditions. *J. Iran. Chem. Res.* 2: 145–149.
- [11] U.G. Akpan, B.H. Hameed. 2012. Parameters Affecting the Photocatalytic Degradation of Dyes Using  $\text{TiO}_2$ -based Photocatalysts: A Review. *J. Hazard. Mater.* 170: 520–529.
- [12] K. Leung, I. M. B. Nielsen, L. J. Criscenti. 2009. Elucidating the Bimodal Acid-base Behavior of the Water-silica Interface from first Principles. *J. Am. Chem. Soc.* 131: 18358–18365.